

Synthesis, characterisation and nonlinear optical properties of tetrahedral clusters $\text{Cp}_2\text{Mo}_2\text{ME}(\text{CO})_7$, ($\text{M} = \text{Fe}, \text{Ru}, \text{Os}$; $\text{E} = \text{S}, \text{Se}$)

Pradeep Mathur ^{a,*}, Sanjukta Ghose ^a, Md. Munkir Hossain ^a, C.V.V. Satyanarayana ^a,
Raj K. Chadha ^b, Sudeep Banerjee ^c, G. Ravindra Kumar ^c

^a Chemistry Department and Regional Sophisticated Instrumentation Centre, Indian Institute of Technology, Powai, Bombay 400 076, India

^b Chemistry Department, BCC159, The Scripps Research Institute, 10555 North Torrey Pines Road, La Jolla, CA 92037, USA

^c Tata Institute of Fundamental Research, Homi Bhabha Road, Bombay 400 005, India

Received 27 April 1998

Abstract

A set of new chalcogen-bridged mixed metal clusters, $\text{Cp}_2\text{Mo}_2\text{M}(\mu_3\text{-E})(\text{CO})_7$, ($\text{M} = \text{Fe}, \text{Ru}, \text{Os}$; $\text{E} = \text{S}, \text{Se}$) have been synthesised and characterised by IR and NMR spectroscopy, and structures of $\text{Cp}_2\text{Mo}_2\text{Ru}(\mu_3\text{-Se})(\text{CO})_7$ and $\text{Cp}_2\text{Mo}_2\text{Os}(\mu_3\text{-Se})(\text{CO})_7$ have been established by single crystal X-ray diffraction methods. The nonlinear optical properties of these clusters were investigated through the Z-scan technique, using 35 ps laser pulses at 532 nm. We report large refractive third order nonlinearity for these clusters indicating their promise for optical limiting applications. © 1998 Elsevier Science S.A. All rights reserved.

Keywords: Tetrahedral clusters; Molybdenum; Iron; Ruthenium; Osmium; Chalcogenide; NLO

1. Introduction

The last decade has witnessed a tremendous development in the chemistry of transition metal clusters stabilised by single atom ligands derived from main group elements [1]. The main group elements act as bridging ligands, thereby serving to maintain the cluster integrity by behaving as a clamp and also help to stabilise the overall cluster framework. Synthesis of these clusters, therefore, continues to attract much attention.

Additional impetus for research on these materials has been provided by the recent investigations of the nonlinear optical properties of clusters in general and of transition metal clusters in particular [2]. It has been shown that exceptionally large third order nonlinearity could be obtained in these clusters [3], making them very attractive for applications in devices based on such effects as optical limiting [4,5]. An attractive aspect of

these materials is the possibility for tailoring the structure to produce a desired nonlinear response [6].

We have recently begun investigations on the nonlinear optical properties of a new class of clusters-mixed metal, mixed chalcogenide clusters [7,8] and have demonstrated that some of these clusters, in particular those containing bridging Se ligands have some of the largest reported nonlinearities till date. These initial investigations have encouraged us to further develop systematic syntheses of chalcogen-bridged mixed-metal clusters and explore the optical nonlinearity of these type of clusters. Such an investigation would contribute towards giving us an insight into the possible cluster core compositions and geometries which are likely to produce good NLO properties.

We have had an extensive and long standing interest in the synthesis and reactivity of such clusters with primary emphasis on the study of the influence of group 16 elements S, Se and Te on the structure, reactivity and bonding pattern of mixed transition metal, non-metal carbonyl clusters [9,10]. The dinuclear

* Corresponding author. Tel.: +91 22 5774089; fax: +91 22 5773480; e-mail: mathur@ether.chem.iitb.ernet.in

and trinuclear compounds, $\text{Fe}_2(\mu\text{-E})_2(\text{CO})_6$ and $\text{Fe}_3(\mu\text{-E})_2(\text{CO})_9$, (E = S, Se, Te) have served as convenient starting materials for such investigations, and systematic synthesis of several classes of mixed-metal clusters have been developed using these compounds.

Recently, we reported the synthesis of $\text{Cp}_2\text{Mo}_2\text{Fe}(\mu_3\text{-Se})(\text{CO})_7$ by the thermolysis of $\text{Fe}_3(\mu_3\text{-Se})_2(\text{CO})_9$ with $\text{Cp}_2\text{Mo}_2(\text{CO})_6$ in benzene solvent [11]. We report here on the designed synthesis of Mo/Group 8 carbonyl clusters of tetrahedral geometry stabilized by the chalcogen ligands, sulfur and selenium, their spectroscopic characterization and crystallographic structure elucidation of two such clusters. We also report on our preliminary investigations of the optical nonlinearity in some of these clusters.

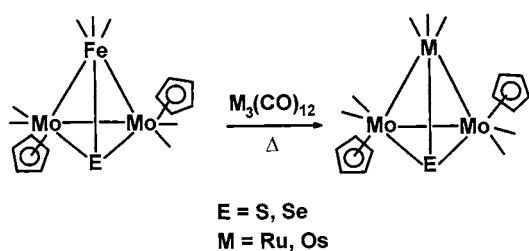
2. Experimental section

2.1. General procedures

All reactions and other manipulations were performed by use of standard Schlenk techniques under an inert atmosphere of nitrogen. All solvents were deoxygenated immediately prior to use. Infrared spectra were recorded on a Nicolet 5DXB or Impact 400 FTIR spectrophotometer as dichloromethane solutions in 0.1 mm path length NaCl cells. Elemental analyses were performed using a Carlo-Erba automatic analyzer. ^1H - and ^{77}Se -NMR spectra were recorded on a Varian VXR-300S spectrometer in CDCl_3 . The operating frequency for ^{77}Se -NMR was 57.23 MHz with a pulse width of 15 μs and a delay of 1 s. The ^{77}Se -NMR spectra are referenced to Me_2Se ($\delta = 0$ ppm). The following compounds $\text{Cp}_2\text{Mo}_2(\text{CO})_6$ [12], $\text{Cp}_2\text{Mo}_2\text{FeS}(\text{CO})_7$ [13], $\text{Cp}_2\text{Mo}_2\text{FeSe}(\text{CO})_7$ [11] and $\text{Cp}_2\text{Mo}_2\text{FeTe}(\text{CO})_7$ [14] were prepared as reported in literature.

2.2. Thermolytic reaction of $\text{Cp}_2\text{Mo}_2\text{FeSe}(\text{CO})_7$ and $\text{Ru}_3(\text{CO})_{12}$

To a benzene solution (75 ml) of $\text{Cp}_2\text{Mo}_2\text{FeSe}(\text{CO})_7$ (30 mg, 0.045 mmol), $\text{Ru}_3(\text{CO})_{12}$ (25 mg, 0.04 mmol) was added and the resulting solution was refluxed



Scheme 1.

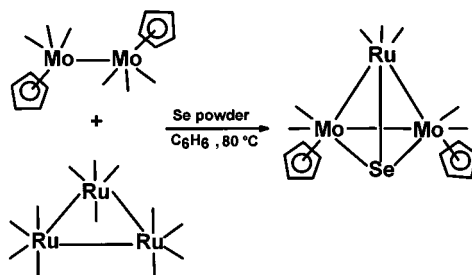
Table 1

Compound	Reactants (mg; mmol)	Yield (%)
$\text{Cp}_2\text{Mo}_2\text{RuSe}(\text{CO})_7$, 1	$\text{Cp}_2\text{Mo}_2(\text{CO})_6$ (200; 0.4) + $\text{Ru}_3(\text{CO})_{12}$ (25; 0.04) + Se powder (10; 0.126)	104 mg (37)
	$\text{Cp}_2\text{Mo}_2\text{FeSe}(\text{CO})_7$ (30; 0.045) + $\text{Ru}_3(\text{CO})_{12}$ (25; 0.04)	9 mg (32)
$\text{Cp}_2\text{Mo}_2\text{RuS}(\text{CO})_7$, 2	$\text{Cp}_2\text{Mo}_2(\text{CO})_6$ (200; 0.4) + $\text{Ru}_3(\text{CO})_{12}$ (25; 0.04) + S powder (10; 0.30)	Nil
	$\text{Cp}_2\text{Mo}_2\text{FeS}(\text{CO})_7$ (25; 0.04) + $\text{Ru}_3(\text{CO})_{12}$ (25; 0.04)	6 mg (23)
$\text{Cp}_2\text{Mo}_2\text{OsSe}(\text{CO})_7$, 3	$\text{Cp}_2\text{Mo}_2(\text{CO})_6$ (200; 0.4) + $\text{Os}_3(\text{CO})_{12}$ (20; 0.022) + Se powder (10; 0.126)	Nil
	$\text{Cp}_2\text{Mo}_2\text{FeSe}(\text{CO})_7$ (30; 0.045) + $\text{Os}_3(\text{CO})_{12}$ (20; 0.022)	8 mg (26)
$\text{Cp}_2\text{Mo}_2\text{OsS}(\text{CO})_7$, 4	$\text{Cp}_2\text{Mo}_2(\text{CO})_6$ (200; 0.4) + $\text{Os}_3(\text{CO})_{12}$ (20; 0.022) + S powder (10; 0.30)	Nil
	$\text{Cp}_2\text{Mo}_2\text{FeS}(\text{CO})_7$ (25; 0.04) + $\text{Os}_3(\text{CO})_{12}$ (20; 0.022)	6 mg (20)

for 24 h (Scheme 1, Table 1). The reaction was closely monitored by TLC and by infrared spectroscopy. The solvent was removed in vacuo, the residue was dissolved in dichloromethane and subjected to chromatographic work-up using silica gel TLC plates. Using 50/50 (v/v) dichloromethane/hexane solvent mixture as eluent, the reddish-brown compound $\text{Cp}_2\text{Mo}_2\text{RuSe}(\text{CO})_7$, **1**, was isolated (9 mg, 32%) together with unreacted $\text{Ru}_3(\text{CO})_{12}$ and $\text{Cp}_2\text{Mo}_2\text{FeSe}(\text{CO})_7$. Several other products were observed during the chromatographic work-up but could not be fully characterized due to insufficient yields. Anal. Calc. for $\text{C}_{17}\text{H}_{10}\text{Mo}_2\text{RuSeO}_7$: C, 29.2; H, 1.43. Found: C, 29.1; H, 1.61.

2.3. Reaction of $\text{Cp}_2\text{Mo}_2(\text{CO})_6$ with $\text{Ru}_3(\text{CO})_{12}$ in presence of Se powder

A mixture of $\text{Cp}_2\text{Mo}_2(\text{CO})_6$ (200 mg, 0.4 mmol), $\text{Ru}_3(\text{CO})_{12}$ (25 mg, 0.04 mmol) and Se powder (10 mg, 0.126 mmol) was refluxed in 150 ml of benzene for 24 h



Scheme 2.

Table 2
Spectroscopic characterisation data for 1–4

Compound	IR (ν_{CO} , cm^{-1}) (in CH_2Cl_2)	$^1\text{H-NMR}$ (C_5H_5)	$^{77}\text{Se-NMR}$
$\text{Cp}_2\text{Mo}_2\text{RuSe}(\text{CO})_7$, 1	2058(s), 1995(vs), 1870(m, br) 1845(m, br)	5.25	394
$\text{Cp}_2\text{Mo}_2\text{RuS}(\text{CO})_7$, 2	2061(s), 1997(vs), 1870(m, br) 1845(m, br)	5.31	—
$\text{Cp}_2\text{Mo}_2\text{OsSe}(\text{CO})_7$, 3	2060(s), 1992(vs), 1862(m, br) 1845(m, br)	5.26	139
$\text{Cp}_2\text{Mo}_2\text{OsS}(\text{CO})_7$, 4	2061(s), 1992(vs), 1870(m, br) 1845(m, br)	5.31	—

with constant stirring (Scheme 2, Table 1). After removal of the solvent in vacuo, the residue was dissolved in dichloromethane and subjected to chromatographic work-up using silica gel TLC plates. Elution with 50/50 (v/v) dichloromethane/hexane mixture afforded the reddish brown compound $\text{Cp}_2\text{Mo}_2\text{RuSe}(\text{CO})_7$, **1**, (104 mg, 37%).

2.4. Reaction of $\text{Cp}_2\text{Mo}_2\text{FeS}(\text{CO})_7$ and $\text{Ru}_3(\text{CO})_{12}$

Thermolysis of a benzene solution (75 ml) of $\text{Cp}_2\text{Mo}_2\text{FeS}(\text{CO})_7$ (25 mg, 0.04 mmol) and $\text{Ru}_3(\text{CO})_{12}$ (25 mg, 0.04 mmol) was carried out for 48 h. The solvent was removed in vacuo, and after dissolving the residue in dichloromethane, chromatographic work-up was carried out using silica gel TLC plates. Elution with 50/50 (v/v) dichloromethane/hexane mixture yielded the orange brown compound $\text{Cp}_2\text{Mo}_2\text{RuS}(\text{CO})_7$, **2**, (6 mg, 23%). Some unreacted $\text{Ru}_3(\text{CO})_{12}$ and $\text{Cp}_2\text{Mo}_2\text{FeS}(\text{CO})_7$ were also isolated from the reaction mixture, together with several other compounds in very low yields which, therefore, could not be fully characterised. Anal. Calc. for $\text{C}_{17}\text{H}_{10}\text{Mo}_2\text{RuSO}_7$: C, 31.3; H, 1.53. Found: C, 31.1; H, 1.71.

2.5. Thermolysis of $\text{Cp}_2\text{Mo}_2\text{FeSe}(\text{CO})_7$ and $\text{Os}_3(\text{CO})_{12}$

To a toluene solution (50 ml) of $\text{Cp}_2\text{Mo}_2\text{FeSe}(\text{CO})_7$ (30 mg, 0.05 mmol), $\text{Os}_3(\text{CO})_{12}$ (20 mg, 0.022 mmol) was added and the solution refluxed for 48 h (Scheme 1). After removal of the solvent in vacuo, the residue was dissolved in dichloromethane and subjected to chromatographic work-up using silica gel TLC plates. On elution with 40/60 (v/v) dichloromethane/hexane mixture, the reddish-brown compound $\text{Cp}_2\text{Mo}_2\text{OsSe}(\text{CO})_7$, **3**, was isolated (8 mg, 26%) together with unreacted $\text{Os}_3(\text{CO})_{12}$ and $\text{Cp}_2\text{Mo}_2\text{FeSe}(\text{CO})_7$. Several other bands were observed in very low yields during the chromatographic separation and hence could not be characterised. Anal. Calc. for $\text{C}_{17}\text{H}_{10}\text{Mo}_2\text{OsSeO}_7$: C, 25.9; H, 1.27. Found: C, 25.6; H, 1.43.

2.6. Thermolysis of $\text{Cp}_2\text{Mo}_2\text{FeS}(\text{CO})_7$ and $\text{Os}_3(\text{CO})_{12}$

A toluene solution (50 ml) of $\text{Cp}_2\text{Mo}_2\text{FeS}(\text{CO})_7$ (25 mg, 0.04 mmol) and $\text{Os}_3(\text{CO})_{12}$ (20 mg, 0.022 mmol) was refluxed for 48 h with constant stirring. The solvent was removed in vacuo. The residue was dissolved in dichloromethane and chromatographic work-up was performed using silica gel TLC plates. Using 40/60 (v/v) dichloromethane/hexane mixture as eluent, a reddish-brown compound $\text{Cp}_2\text{Mo}_2\text{OsS}(\text{CO})_7$, **4**, (6 mg, 20%) was obtained together with some amount of unreacted $\text{Os}_3(\text{CO})_{12}$ and $\text{Cp}_2\text{Mo}_2\text{FeS}(\text{CO})_7$. Several other bands were observed during chromatographic work-up, but could not be fully characterised due to insufficient yields. Anal. Calc. for $\text{C}_{17}\text{H}_{10}\text{Mo}_2\text{OsSO}_7$: C, 27.6; H, 1.35. Found: C, 27.3; H, 1.62.

2.7. Reaction of $\text{Cp}_2\text{Mo}_2\text{FeS}(\text{CO})_7$ with Se powder

A benzene solution (75 ml) of $\text{Cp}_2\text{Mo}_2\text{FeS}(\text{CO})_7$ (25 mg, 0.04 mmol) and Se powder (10 mg, 0.126 mmol) was refluxed for 36 h with constant stirring. The reaction was closely monitored by IR spectroscopy and thin layer chromatography. Formation of the Se containing tetrahedron cluster $\text{Cp}_2\text{Mo}_2\text{FeSe}(\text{CO})_7$ from the parent S-containing cluster was not observed.

2.8. Reaction of $\text{Cp}_2\text{Mo}_2\text{RuSe}(\text{CO})_7$ and $\text{Os}_3(\text{CO})_{12}$

To a toluene solution (50 ml) of $\text{Cp}_2\text{Mo}_2\text{RuSe}(\text{CO})_7$ (20 mg, 0.03 mmol), $\text{Os}_3(\text{CO})_{12}$ (25 mg, 0.03 mmol) was added and the solution refluxed for 36 h with constant stirring. The reaction was monitored by thin layer chromatography and IR spectroscopy. Formation of the compound $\text{Cp}_2\text{Mo}_2\text{OsSe}(\text{CO})_7$ was not observed.

2.9. Crystal structure determination of **1** and **3**

Crystals of compounds **1** and **3**, suitable for X-ray diffraction analysis were grown from hexane and dichloromethane solvent mixtures by slow evaporation of the solvents at 0°C . The crystal with the largest dimension was mounted and data were collected with a Rigaku AFC6S diffractometer equipped with a sealed molybdenum tube and a highly oriented graphite

monochromator. A constant scan speed of 8° min^{-1} in ω was used and weak reflections [$I < 5\sigma(I)$] were rescanned to a maximum of four times and the counts were accumulated to assure good counting statistics. The intensities of three monitor reflections measured after every 150 reflections did not change significantly during the 36 h of X-ray exposure. Unit cell dimensions and standard deviations were obtained by least-squares fit to 25 reflections ($20 < 2\theta < 40^\circ$). The data were corrected for Lorentz and polarization effects and an absorption correction based on a Ψ -scan was also applied. The structure was solved by direct methods using SHELXS86. The refinement was done by full-ma-

trix least-squares $n F^2$. The function minimized was $\Sigma w(|F_o| - |F_c|)^2$. Hydrogen atoms were included in the ideal positions with a fixed isotropic U value of 0.082 \AA^2 . All calculations were done on a Silicon graphics Personal Iris 4D/35 and an IBM compatible PC using programs TEXSAN (data reduction), SHELXL-93 (refinement) and SHELXTL (plotting).

In case of compound **1**, the systematic absences (hkl , $h + k = 2n + 1$; and $h0l$, $l = 2n + 1$) indicated the space group to be $C2/c$. All non-hydrogen atoms were refined anisotropically by the full-matrix least-squares method. In this case, a weighting scheme of the form $w = 1/[\sigma^2(F_o^2) + (aP)^2 + bP]$ with $a = 0.067$ and $b = 38.42$ was used. (P is defined as $\max(F_o^2, 0) + 2F_c^2/3$). An extinction correction was also applied to the data.

For compound **3**, the systematic absences ($h00$, $h = 2n + 1$; $0k0$, $k = 2n + 1$; and $00l$, $l = 2n + 1$) indicated that the space group was $P2_12_12_1$. Os, Se, Mo and O atoms were refined anisotropically and C atoms isotropically by the full-matrix least-squares method. A weighting scheme of the form $w = 1/[\sigma^2(F_o^2) + (aP)^2 + bP]$ with $a = 0.08$ and $b = 97.58$ was used. (P is defined as $\max(F_o^2, 0) + 2F_c^2/3$). There was no evidence of secondary extinction; therefore it was not applied.

The refinement for both **1** and **3** converged to the R indices given in Table 3 which also includes the largest difference peak and the hole in the last cycles of refinement. The final difference map was devoid of significant features.

2.10. Studies on nonlinear optical properties

The linear absorption spectra of the solutions of the clusters in n -hexane were obtained using a UV-vis spectrometer and their third order susceptibility (χ^3) by the Z-scan technique [15]. The frequency doubled output ($\lambda = 532 \text{ nm}$) of an active-passive modelocked Nd-YAG laser was focussed on the sample using a lens. The laser emitted 35 ps pulses at a repetition rate of 10 Hz. A half-wave plate and polariser combination was placed in the beam path to vary the input energy. The solution of sample in n -hexane, placed in a 1 mm quartz cuvette, was moved along the beam axis by a precision translation stage. The incident energy and the transmitted energy through the samples were monitored by sensitive photodiodes and the signals were averaged using a digital storage oscilloscope. To minimise irradiance fluctuations a single channel analyser was used to trigger the data acquisition system only when the incident energy was within $\pm 5\%$ of a preset value. The nonlinear attenuation of the input laser beams results from the modification of the refractive index and the absorption coefficient via the third order susceptibility, χ^3 . The modified refractive index is given by $n = n_0 + \gamma I$ and the absorption coefficient by $\alpha = \alpha_0 + \beta I$; n_0 and α_0 being the values in the linear regime. The parameters γ

Table 3
Crystal data and structure refinement details for **1** and **3**

	Compound 1	Compound 3
Empirical formula	$\text{C}_{17}\text{H}_{10}\text{Mo}_2\text{O}_7\text{RuSe}$	$\text{C}_{17}\text{H}_{10}\text{Mo}_2\text{O}_7\text{OsSe}$
Formula weight	698.16	787.29
Wavelength (\AA)	0.71073	0.71073
Temperature (K)	296(2)	296(2)
Crystal dimensions (mm)	$0.31 \times 0.22 \times 0.14$	$0.29 \times 0.16 \times 0.12$
Crystal system	Monoclinic	Orthorhombic
Space group	$C2/c$	$P2_12_12_1$
Lattice parameters		
a (\AA)	31.017(6)	9.280(2)
b (\AA)	8.614(2)	13.248(3)
c (\AA)	15.152(3)	15.923(3)
α ($^\circ$)	90	90
β ($^\circ$)	103.18(3)	90
γ ($^\circ$)	90	90
V (\AA^3)	3941.7(14)	1957.6(7)
Z	8	4
$F(000)$	2640	1448
D_{calc} (mg m^{-3})	2.353	2.671
Absorption coefficient (mm^{-1})	3.893	9.632
Data collection range for θ ($^\circ$)	2.46–25.02	2.54–25.05
Scan type	$2\theta - \theta$	$2\theta - \theta$
Index ranges	$0 \leq h \leq 36, 0 \leq k \leq 10, 18 \leq l \leq 17$	$0 \leq h \leq 10, 0 \leq k \leq 14, 0 \leq l \leq 17$
No. of reflections collected	3889	1807
No. of independent reflections, ($R_{\text{int}} = 0.000$)	3472	1749
No of data/restraints/parameters	3457/0/254	1727/1/168
Goodness-of-fit on F^2 , (S)	1.012	1.113
Final R indices ($I > 2\sigma(I)$)	$R_1 = 0.0393, wR_2 = 0.1009$	$R_1 = 0.0556, wR_2 = 0.1379$
Final R indices (all data)	$R_1 = 0.0804, wR_2 = 0.1968$	$R_1 = 0.0926, wR_2 = 0.3718$
Extinction coefficient	0.00105(8)	—
Flack's absolute structural parameter	—	-0.04(3)
Largest diffracting peak/hole (e \AA^{-3})	0.944/-0.932	2.295/-3.707

$$R_1 = (\Sigma ||F_o| - |F_c||) / \Sigma |F_o|, wR_2 = \Sigma w (F_o^2 - F_c^2)^2 / \Sigma w [(F_o^2)^2]^{1/2}, S = [\Sigma w (F_o^2 - F_c^2)^2 / (n-p)]^{1/2}.$$

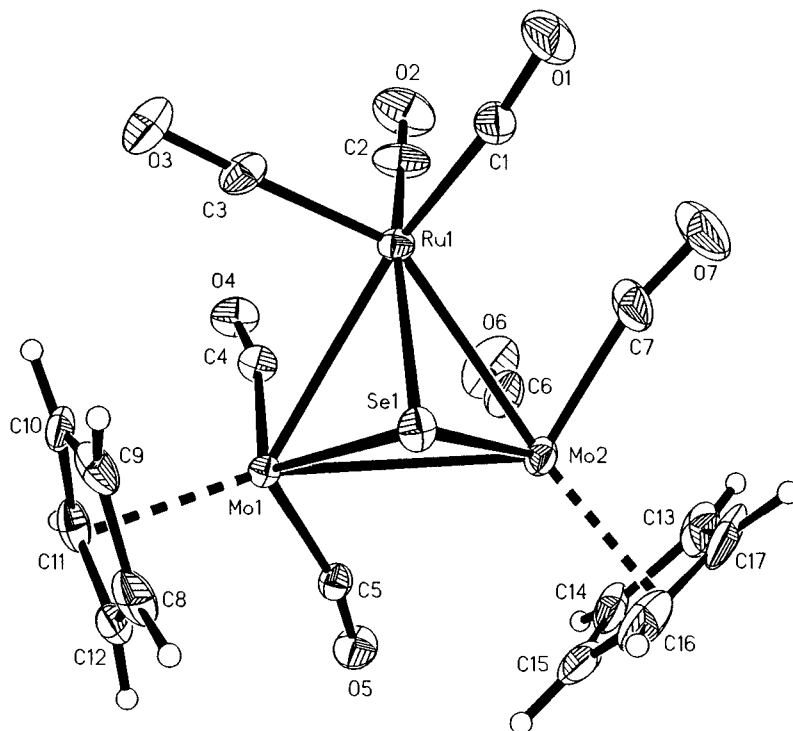


Fig. 1. ORTEP view of $\text{Cp}_2\text{Mo}_2\text{RuSe}(\text{CO})_7$. The atoms are drawn with 30% probability ellipsoids.

and β are the coefficients of nonlinear refraction and absorption, respectively, and I is the laser intensity. To measure γ an aperture was inserted in the transmitted beam (closed aperture scan) and a fraction of the output light was collected. The measurement of β involves collecting all of the transmitted light (open aperture scan) using a large aperture lens. In our experiments a beam splitter was introduced in the transmitted beam and the open and closed aperture scans were performed simultaneously. The experimental data on nonlinear refraction has been fitted to the model of Sheik-Bahae et al. to obtain γ and β [15].

3. Results and discussion

3.1. Synthesis

The thermolysis of a benzene solution of $\text{Cp}_2\text{Mo}_2\text{FeSe}(\text{CO})_7$ and $\text{Ru}_3(\text{CO})_{12}$ for 24 h, afforded the reddish-brown compound $\text{Cp}_2\text{Mo}_2\text{RuSe}(\text{CO})_7$, **1**, in 32% yield (Scheme 1). Compound **1** was also isolated in a yield of 37%, when a mixture of $\text{Cp}_2\text{Mo}_2(\text{CO})_6$ and $\text{Ru}_3(\text{CO})_{12}$ was refluxed in benzene for 24 h in presence of Se powder (Scheme 2, Table 1). Similarly, when benzene solution of $\text{Cp}_2\text{Mo}_2\text{FeS}(\text{CO})_7$ and $\text{Ru}_3(\text{CO})_{12}$, or toluene solution of $\text{Cp}_2\text{Mo}_2\text{FeSe}(\text{CO})_7$ and $\text{Os}_3(\text{CO})_{12}$ were refluxed, $\text{Cp}_2\text{Mo}_2\text{RuS}(\text{CO})_7$, **2** (23% yield), and $\text{Cp}_2\text{Mo}_2\text{OsSe}(\text{CO})_7$ **3** (26% yield), respec-

tively were obtained. Cluster **2** has previously been obtained from the thermolysis reaction of $\text{Cp}_2\text{Mo}_2(\text{CO})_6$ with $\text{CpMoRuCo}(\mu_3\text{-S})(\text{CO})_9$ [13], and of $\text{Cp}_2\text{Mo}_2(\text{CO})_4$ with $\text{Ru}_3(\text{CO})_9(\mu_3\text{-CO})(\mu_3\text{-S})$ [16]. The reddish-brown compound, $\text{Cp}_2\text{Mo}_2\text{OsS}(\text{CO})_7$, **4** was formed likewise, with a yield of 20%, when a toluene solution of $\text{Cp}_2\text{Mo}_2\text{FeS}(\text{CO})_7$ and $\text{Os}_3(\text{CO})_{12}$ was refluxed.

Unreacted starting materials were recovered from all the reactions. Several other compounds were observed during the chromatographic work-up of all reactions, but these could not be fully characterised due to insufficient yields.

Formation of **1–4** takes place by atom transfer reactions, where the smaller Fe atom in $\text{Cp}_2\text{Mo}_2\text{Fe}(\text{CO})_7$ is formally replaced by Ru or Os atom. Atom transfer reactions have previously been used as a means to produce new clusters, and have occasionally resulted in increase in nuclearity, as for instance in the thermolytic reaction between $\text{Fe}_3(\text{CO})_9(\mu_3\text{-Te})_2$ and $\text{Ru}_3(\text{CO})_{12}$ to form $\text{Ru}_4(\text{CO})_{11}(\mu_4\text{-Te})_2$ [17]. Metal exchange reactions have been applied successfully in the case of sulfido-bridged clusters, $\text{SFeCo}_2(\text{CO})_9$, and $\text{SMCo}_2(\text{CO})_9$ to yield the mixed-metal clusters, $\text{SFeCoMCp}(\text{CO})_8$ ($\text{M} = \text{Cr}, \text{Mo}, \text{W}$) and $\text{SRuCoMCp}(\text{CO})_8$ ($\text{M} = \text{Mo}, \text{W}$) [13]. Formation of **1–4** by such type of reactions provides a convenient route to examine the effect of variation of a single vertex on a tetrahedral core geometry of a cluster on its properties.

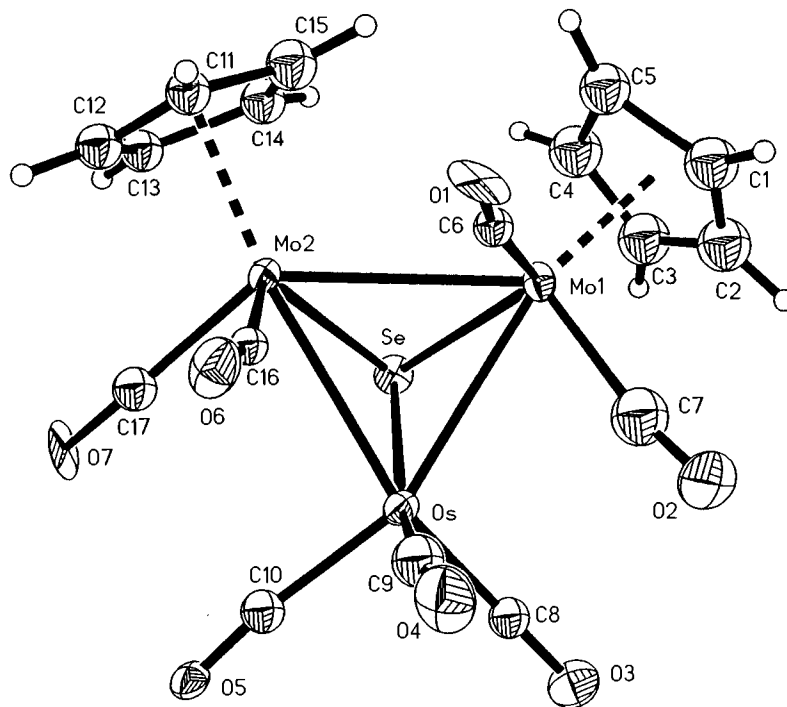


Fig. 2. ORTEP view of $\text{Cp}_2\text{Mo}_2\text{OsSe}(\text{CO})_7$. The atoms are drawn with 30% probability ellipsoids.

3.2. Spectroscopic characterization

The compounds **1–4** have been characterized by IR, and ^1H - and ^{77}Se -NMR spectroscopy. The spectroscopic data are summarized in Table 2. All four compounds were stable both in the solid state and in solution. The solution IR spectrum of all compounds reveals identical CO stretching pattern, indicating the

presence of only terminally bonded carbonyl ligands. The ^1H -NMR spectra shows one sharp signal in the range δ 5.2–5.3 ppm, which can be attributed to the two equivalent Cp ligands in each compound. The ^{77}Se -NMR spectra of **1** and **3** show a single sharp peak in the range generally observed for a triply bridging Se atom, δ 796.4 ppm in $\text{CpCoFe}_2(\text{CO})_6(\mu_3\text{-Se})_2$ [18]; δ 737.8 ppm in $\text{CpCoFe}_2(\text{CO})_6(\mu_3\text{-S})(\mu_3\text{-Se})$ [18]; δ 659 ppm in $\text{Cp}_2\text{Mo}_2\text{Fe}_2(\text{CO})_6(\mu_4\text{-Te})(\mu_3\text{-Se})(\mu_3\text{-S})$ [14].

Table 4
Selected bond lengths (Å) and angles (°) for **1** and **3**

	Compound 1	Compound 3
Mo(1)–Mo(2)	3.099(1)	3.032(6)
Mo(1)–Se	2.510(1)	2.520(5)
Mo(2)–Se	2.519(1)	2.526(5)
Ru–Se	2.4472(12)	—
Os–Se	—	2.450(4)
Ru–Mo(1)	2.8935(11)	—
Ru–Mo(2)	2.9210(13)	—
Os–Mo(1)	—	2.917(4)
Os–Mo(2)	—	2.946(3)
Mo(1)–Se–Mo(2)	76.09(4)	73.8(1)
Mo(1)–Ru–Mo(2)	64.41(3)	—
Mo(1)–Os–Mo(2)	—	62.25(9)
Ru–Se–Mo(1)	71.41(3)	—
Ru–Se–Mo(2)	72.04(4)	—
Os–Se–Mo(1)	—	71.85(13)
Os–Se–Mo(2)	—	72.57(13)
Se–Ru–Mo(1)	55.30(3)	—
Se–Ru–Mo(2)	55.12(3)	—
Se–Os–Mo(1)	—	55.18(12)
Se–Os–Mo(2)	—	54.90(11)

3.3. Molecular structures

The molecular structures of **1** and **3**, elucidated by single crystal X-ray diffraction analysis, are shown in Figs. 1 and 2, respectively. The crystal data and refinement details are summarized in Table 3, and selected bond lengths and bond angles for **1** and **3** are given in Table 4. Atomic coordinates and equivalent isotropic displacement parameters for **1** and **3** are listed in Tables 5 and 6, respectively. Clusters **1** and **3** are isostructural; the cluster core consists of a Mo_2MSe tetrahedron (**1**, $\text{M} = \text{Ru}$; **3**, $\text{M} = \text{Os}$) with each Mo atom having two terminally bonded carbonyl groups and one $\eta^5\text{-Cp}$ group attached to it. Three other terminal CO ligands are present on the Ru/Os atom. The average Mo–Ru bond distance in **1**, 2.9072 Å is very similar to that observed in the sulfido-bridged cluster, **2** (2.9059 Å) [16]. The Ru–Se bond length (2.4472(12) Å) in **1** is shorter than the Ru–Se bond distances observed in the square pyramidal cluster, $\text{Ru}_3(\text{CO})_9(\mu_3\text{-Se})_2$ (av. Ru(basal)–Se, 2.483 Å; av. Ru(apical)–Se, 2.521 Å)

Table 5

Atomic coordinates ($\times 10^4$) and equivalent isotropic displacement parameters ($\text{\AA} \times 10^3$) for **1**

Atom	x	y	z	U_{eq}
Ru(1)	3800(1)	2195(1)	3244(1)	35(1)
Mo(1)	3248(1)	3860(1)	4228(1)	30(1)
Mo(2)	4195(1)	2770(1)	5157(1)	42(1)
Se(1)	3970(1)	4765(1)	3923(1)	40(1)
O(1)	4504(3)	1947(12)	2151(6)	90(3)
O(2)	3612(3)	-1258(11)	3132(7)	96(3)
O(3)	3096(3)	2849(11)	1548(5)	81(3)
O(4)	2873(2)	501(8)	3932(5)	60(2)
O(5)	3308(2)	3300(10)	6264(4)	63(2)
O(6)	3776(4)	-453(11)	5395(6)	103(4)
O(7)	4850(4)	1035(16)	4255(6)	131(5)
C(1)	4261(3)	2068(13)	2601(7)	54(3)
C(2)	3680(4)	25(12)	3192(7)	62(3)
C(3)	3362(4)	2628(13)	2196(6)	53(3)
C(4)	3062(3)	1676(11)	4042(6)	43(2)
C(5)	3334(3)	3482(11)	5523(6)	41(2)
C(6)	3918(4)	718(14)	5270(7)	62(3)
C(7)	4577(4)	1668(18)	4496(8)	81(4)
C(8)	2972(4)	6389(12)	4054(9)	67(3)
C(9)	2900(4)	5715(13)	3175(7)	60(3)
C(10)	2615(3)	4506(13)	3176(8)	59(3)
C(11)	2511(3)	4431(13)	4030(9)	60(3)
C(12)	2719(3)	5594(13)	4544(7)	55(3)
C(13)	4695(4)	2186(21)	6421(8)	87(5)
C(14)	4325(4)	2771(18)	6708(7)	68(4)
C(15)	4295(4)	4309(18)	6459(8)	73(4)
C(16)	4611(5)	4759(22)	6020(9)	92(5)
C(17)	4873(4)	3432(28)	6019(8)	103(6)

Table 6

Atomic coordinates ($\times 10^4$) and equivalent isotropic displacement parameters ($\text{\AA} \times 10^3$) for **3**

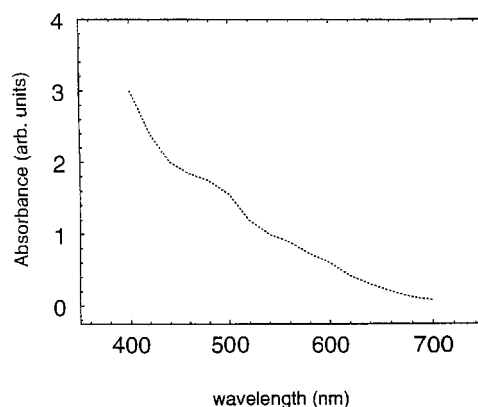
Atom	x	y	z	U_{eq}
Os	8147(2)	4359(1)	5685(1)	36(1)
Mo(1)	5626(4)	5250(2)	4880(2)	38(1)
Mo(2)	5346(3)	4142(2)	6538(2)	34(1)
Se	6089(4)	3402(3)	5141(3)	43(1)
O(1)	5483(37)	6887(22)	6296(21)	75(10)
O(2)	8400(39)	6424(24)	4393(34)	111(16)
O(3)	10101(34)	4069(25)	4175(20)	71(9)
O(4)	9767(42)	6184(30)	6403(24)	91(12)
O(5)	9809(30)	2839(21)	6705(19)	53(8)
O(6)	7185(34)	5551(27)	7617(19)	76(10)
O(7)	6921(44)	2339(21)	7399(20)	77(10)
C(1)	4471(65)	6320(47)	3965(36)	86(17)
C(2)	5112(64)	5694(46)	3480(38)	90(17)
C(3)	4625(66)	4759(46)	3569(40)	92(17)
C(4)	3554(66)	4762(48)	4134(37)	94(19)
C(5)	3353(55)	5798(38)	4490(32)	78(14)
C(6)	5567(40)	6202(27)	5803(24)	41(8)
C(7)	7487(66)	5877(47)	4534(38)	93(18)
C(8)	9347(43)	4165(31)	4746(26)	51(10)
C(9)	9120(55)	5417(38)	6162(31)	68(13)
C(10)	9114(49)	3344(35)	6336(29)	56(11)
C(11)	3576(46)	4823(34)	7363(28)	55(11)
C(12)	3848(49)	3917(33)	7662(26)	63(12)
C(13)	3404(45)	3211(36)	7030(27)	58(11)
C(14)	2889(49)	3825(35)	6304(30)	63(12)
C(15)	2973(53)	4729(37)	6506(27)	74(14)
C(16)	6653(40)	5019(28)	7114(23)	39(8)
C(17)	6387(48)	3033(37)	7106(30)	60(12)

[19]. The Mo–Mo bond distances are almost identical for M = Fe (3.096(1)) [11], Ru (**1**) (3.099(1)) and Os (**3**) (3.032(6)) in $\text{Cp}_2\text{Mo}_2\text{MSe}(\text{CO})_7$. The Mo–Ru–Mo (64.41(3)°) and Mo–Se–Mo (76.09(4)°) bond angles in **1** are both slightly larger than the Mo–Os–Mo (62.25(9)°) and Mo–Se–Mo (73.882(14)°) bond angles in **3**. The average Se–M–Mo bond angles, where M = Ru (**1**) or Os (**2**), are comparable, (55.2° in **1** and 55.0° in **3**), and slightly smaller than that observed earlier in $\text{Cp}_2\text{Mo}_2\text{FeSe}(\text{CO})_7$ (57.2°) [11]. The Os–Se bond distance in **3** (2.450(4) Å) is shorter than the average Os–Se bond distances observed in $\text{Os}_3(\text{CO})_9\text{Se}_2$ (2.517 Å) [20] and $\text{H}_2\text{Os}_4(\text{CO})_{12}\text{Se}_2$ (2.5518 Å) [21].

3.4. Nonlinear optical properties of $\text{Cp}_2\text{Mo}_2\text{FeSe}(\text{CO})_7$ and **1** and **3**

The absorption spectra of one of the clusters, $\text{Cp}_2\text{Mo}_2\text{SeFe}(\text{CO})_7$ is shown in Fig. 3. It is evident that absorption at 532 nm is quite small and that it increases towards the shorter wavelength region. Absorption spectra of the other two clusters were similar in their behaviour to the one shown here. Fig. 4 shows the results of the Z-scan study for $\text{Cp}_2\text{Mo}_2\text{SeFe}(\text{CO})_7$ at a peak (at focus) intensity of 2.1 GWcm^{-2} . The linear

absorption coefficient of the solution was 3.4 cm^{-1} at 532 nm. The refractive nonlinearity (closed aperture Z-scan) was found to be considerable, as evident in the peak-valley separation in Fig. 4. The solid curve in the figure is a theoretical fit based on the model of Sheik-Bahae et al. [15], assuming that the nonlinearity is mainly of third order. The peak to valley change in the transmission is close to 1.0, indicating a large refractive nonlinearity, with a γ of $-2.2 \times 10^{-12} \text{ cm}^2 \text{ W}^{-1}$. Moreover, the negative value of γ indicates that for the

Fig. 3. UV-vis absorption spectra of $\text{Cp}_2\text{Mo}_2\text{SeFe}(\text{CO})_7$ in *n*-hexane

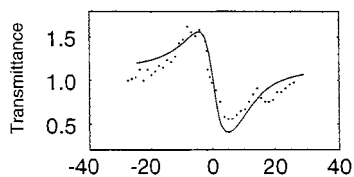


Fig. 4. Z-scan of $\text{Cp}_2\text{Mo}_2\text{SeFe}(\text{CO})_7$ in *n*-hexane. The filled circles are the experimentally measured data points while the solid curve is a theoretical fit.

$\text{Cp}_2\text{Mo}_2\text{SeFe}(\text{CO})_7$ cluster, the nonlinearity is of the self-defocussing type. The good agreement between fit and the data justifies the assumption of a predominantly third order nonlinearity. None of the clusters displayed measurable absorptive (open aperture) nonlinearity at this wavelength, at the laser intensity used in this study. The mechanism responsible for the large refractive nonlinearity needs to be understood, particularly because it is not accompanied by a significant absorptive counterpart, as in the case of many other clusters. Shi et al. [22] have reported similar behaviour in $\text{WCu}_2\text{OS}_3(\text{PPh}_3)_4$, though the nonlinearity measured is considerably smaller. We are in the process of modelling the nonlinear response of the clusters reported upon in this study.

The nonlinearity of $\text{Cp}_2\text{Mo}_2\text{SeFe}(\text{CO})_7$ is superior to that found at the same wavelength for C_{60} ($-9.0 \times 10^{-13} \text{ cm}^2 \text{ W}^{-1}$) which is often used as the benchmark optical limiter [23]. The other two clusters display nonlinearity similar to that of C_{60} . It is thus obvious that the present clusters may serve as efficient optical limiters. Also, it is noteworthy to note that the clusters display no absorptive nonlinearity. We are investigating this aspect further.

Acknowledgements

Financial grant to P. Mathur by the Board of Research on Nuclear Sciences, Government of India, is gratefully acknowledged. S. Ghose thanks the Council of Scientific and Industrial Research, Government of India, for the award of a Senior Research Fellowship.

References

- [1] (a) K.H. Whitmire, *J. Coord. Chem.* 17 (1988) 95. (b) L. Linford, H.G. Raubenheimer, *Adv. Organomet. Chem.* 32 (1991) 1. (c) M.A. Ansari, J.A. Ibers, *Coord. Chem. Rev.* 100 (1990) 223. (d) L.C. Roof, J.W. Kolis, *Chem. Rev.* 93 (1993) 1037.
- [2] (a) L.W. Tutt, S.W. McCahon, *Optics Lett.* 15 (1990) 700. (b) Z.R. Chen, H.R. Hou, X.Q. Xin, K.B. Yu, S. Shi, *J. Phys. Chem.* 99 (1995) 8717. (c) W. Ji, S. Shi, H.J. Du, P. Ge, S.H. Tang, X.Q. Xin, *J. Phys. Chem.* 99 (1995) 17297.
- [3] (a) S. Shi, W. Ji, X.Q. Xin, *J. Phys. Chem.* 99 (1995) 894. (b) H. Hou, B. Liang, X. Xin, K. Yu, P. Ge, W. Ji, S. Shi, *J. Chem. Soc. Faraday Trans.* 92 (1996) 2343. (c) P. Ge, S.H. Tang, W. Ji, S. Shi, H.W. Hou, D.L. Long, X.Q. Xin, S.F. Liu, Q.J. Wu, *J. Phys. Chem.* 101 (1997) 27.
- [4] L.W. Tutt, T.F. Boggess, *Prog. Quantum Electron.* 17 (1993) 299.
- [5] L.W. Tutt, A. Kost, *Nature* 356 (1992) 225.
- [6] J.L. Bredas, C. Adant, P. Tackx, A. Persoons, B.M. Pierce, *Chem. Rev.* 94 (1994) 243.
- [7] S. Banerjee, G.R. Kumar, P. Mathur, P. Sekar, *Chem. Comm.* (1997) 299.
- [8] P. Mathur, S. Ghose, M.M. Hossain, C.V.V. Satyanarayana, S. Banerjee, G.R. Kumar, P.B. Hitchcock, J.F. Nixon, *Organometallics* 16 (1997) 3815.
- [9] P. Mathur, *Adv. Organomet. Chem.* 41 (1997) 243.
- [10] P. Mathur, D. Chakrabarty, I.J. Mavunkal, *J. Clust. Sci.* 4 (1993) 351.
- [11] P. Mathur, M.M. Hossain, A.L. Rheingold, *Organometallics* 13 (1994) 3909.
- [12] D.S. Ginley, C.R. Bock, M.S. Wrighton, *Inorg. Chim. Acta.* 23 (1977) 85.
- [13] F. Richter, E. Roland, H. Vahrenkamp, *Chem. Ber.* 117 (1984) 2429.
- [14] P. Mathur, M.M. Hossain, S.B. Umbarkar, C.V.V. Satyanarayana, A.L. Rheingold, L.M. Liable-Sands, G.P.A. Yap, *Organometallics* 15 (1996) 1898.
- [15] M. Sheik-Bahae, A.A. Said, T.H. Wei, D.J. Hagan, E.W. Van Stryland, *IEEE J. Quantum Electron.* 26 (1990) 760.
- [16] R.D. Adams, J.E. Babin, M. Tasi, *Organometallics* 7 (1988) 219.
- [17] P. Mathur, B.H.S. Thimmappa, A.L. Rheingold, *Inorg. Chem.* 29 (1990) 4658.
- [18] P. Mathur, P. Sekar, C.V.V. Satyanarayana, M.F. Mahon, *Organometallics* 14 (1995) 2115.
- [19] T.M. Layer, J. Lewis, A. Martin, P.R. Raithby, W.T. Wong, *J. Chem. Soc. Dalton Trans.* (1992) 3411.
- [20] B.F.G. Johnson, J. Lewis, P.G. Lodge, P.R. Raithby, *Acta Crystallogr.* 37B (1981) 1731.
- [21] B.F.G. Johnson, J. Lewis, P.G. Lodge, P.R. Raithby, K. Henrick, M. McPartlin, *Chem. Commun.* (1979) 719.
- [22] S. Shi, H.W. Hou, X.Q. Xin, *J. Phys. Chem.* 99 (1995) 4050.
- [23] S. Couris, E. Koudomas, A.A. Ruth, S. Leach, *J. Phys. B* 28 (1995) 4537.